

# Sol–gel phase transition induced by fiber–vesicle structural changes in sugar-based bolaamphiphiles

2 PERKIN

Hideki Kobayashi,<sup>a</sup> Kazuya Koumoto,<sup>a</sup> Jong Hwa Jung<sup>a</sup> and Seiji Shinkai<sup>\*a,b</sup>

<sup>a</sup> Chemotransfiguration project, Japan Science and Technology Corporation (JST), 2432 Aikawa, Kurume, Fukuoka 839-0861, Japan

<sup>b</sup> Department of Chemistry and Biochemistry, Graduate School of Engineering, Kyushu University, Fukuoka 812-8581, Japan

Received (in Cambridge, UK) 13th May 2002, Accepted 19th August 2002  
First published as an Advance Article on the web 2nd October 2002

The research objects of this paper were to design bolaamphiphilic gelators utilizing a sugar family as a source of solvophilic groups and an azobenzene segment as a solvophobic group and to monitor the aggregation mode utilizing the spectroscopic properties of the azobenzene chromophore. The results indicated that the bolaamphiphiles act, although only for specific DMSO–water mixtures, as gelators and form a unique supramolecular helical structure in the gel phase. The UV-Vis and CD spectra showed that the azobenzene segments adopt H-type face-to-face orientation and the dipole moments are arranged in the right-handed (*R*)-helicity. Since the fibrils as observed by electron microscope possess the right-handed helical structure, one may consider that the microscopic azobenzene–azobenzene orientation is reflected by the macroscopic supramolecular structure. When boronic acid-appended poly(L-lysine) was added, the gel phase was changed into the sol phase in the macroscopic level and the fibrous aggregate was changed into the vesicular aggregate in the microscopic level. These changes, which are usually induced by a temperature change, are due to the specific boronic acid–sugar interaction occurring at the constant temperature. Interestingly, when D-fructose which shows high affinity with the boronic acid group was added, the sol phase and the vesicular aggregate were changed back to the gel phase and the fibrous aggregate, respectively. This means that the phase and morphological changes in the sugar-integrated bolaamphiphiles can be controlled reversibly.

## Introduction

Organogels are thermoreversible, viscoelastic materials consisting of low molecular weight compounds self-assembled into complex three-dimensional structures.<sup>1</sup> Multiple non-covalent interactions such as hydrogen bonding, donor–acceptor and hydrophobic interactions between the organogel building blocks are responsible for the gel-forming process. Although many examples of gelators for organic solvents have been reported in the literature, fewer studies on gelators for water (hydrogelators) have been presented so far.<sup>2</sup> The development of strong, thermoreversible hydrogelators can lead to new useful materials for drug delivery, wound healing and tissue engineering processes.<sup>3</sup> In our group we have synthesized and studied a variety of simple sugar-based compounds that are able to gelate water, organic solvents, or both.<sup>4,5</sup> We, as well as others, have noticed that hydrophobic interactions, for example in the form of aromatic  $\pi$ – $\pi$  stacking, are indispensable for the formation of oriented aggregates in water and are most probably the initial driving force for the self-assembly process.<sup>1,2</sup> Furthermore, hydrogen bonding also seems to play a role in the orientation of the molecules within the aggregates. For example, we already have found that acetylated sugar-integrated gelator could not act as a ‘supergelator’ in water and organic solvents,<sup>5</sup> indicating that hydrogen bonding is important to form ‘supergelators’ in water as well as organic solvents.

It is known that boronic acid form complexes with diol-type hydroxyl groups of carbohydrate *via* ester-linkage formation.<sup>6</sup> In particular, our and other groups have intensively developed new aspects on aqueous sugar sensing by employing aromatic boronic acids.<sup>7–9</sup> These studies tell us that if this concept is applied to the gel system utilizing sugar-integrated gelators, gelation properties such as gelation ability, sol–gel phase transition temperature ( $T_{\text{gel}}$ ) and morphological changes could be

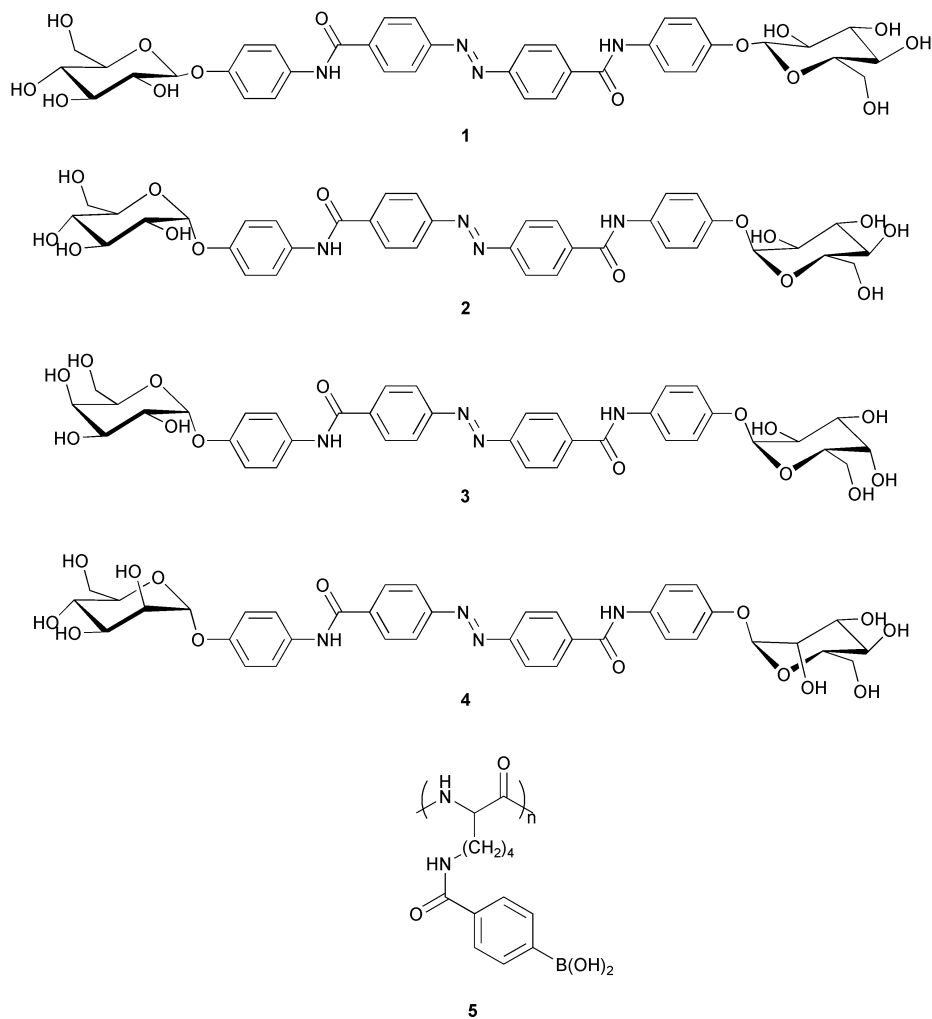
controlled by boronic acid-based additives. For example, we found that the gelation ability of a sugar-based gelator dramatically changes in the presence of boronic acid-appended poly(L-lysine),<sup>10</sup> which dramatically enhances  $T_{\text{gel}}$ .<sup>11</sup> This approach might be useful as a strategy to control novel supramolecular aggregate structures in the presence of boronic acid derivatives.

With these objects in mind, we designed  $\beta$ -D-glucose-based **1**,  $\alpha$ -D-glucose-based **2**,  $\alpha$ -D-galactose-based **3** and  $\alpha$ -D-mannose-based **4**, each of which has two aminophenyl sugar skeletons as a chiral aggregate-forming site producing a hydrophilic driving force and one azobenzene moiety as a  $\pi$ – $\pi$  stacking site producing a hydrophobic driving force (Scheme 1). In this work, we have found that the  $T_{\text{gel}}$  and the morphologies of the sugar-integrated gels are profoundly affected by the structure of the sugar moieties. The fibrous aggregate constructed in the gel phase was easily converted into a vesicular aggregate in the presence of boronic acid-appended poly(L-lysine). More interestingly, when D-fructose which shows high affinity with the boronic acid group, was added the vesicular aggregate was changed back to the fibrous aggregate. As a result, the sol–gel phase transition in the sugar-integrated bolaamphiphiles can be controlled reversibly using boronic acid-appended poly(L-lysine) and D-fructose. To the best of our knowledge, this is the first study of morphology control in gel systems by addition of boronic acid-appended poly(L-lysine) and D-fructose.

## Results and discussion

### Spectral characterization in solution

To obtain basic spectroscopic information on the monomeric and aggregate states of these amphiphiles, their UV-Vis and CD spectra were measured in DMSO–water mixtures. As a typical example, the UV-Vis spectra of **4** are shown in Fig. 1.



Scheme 1

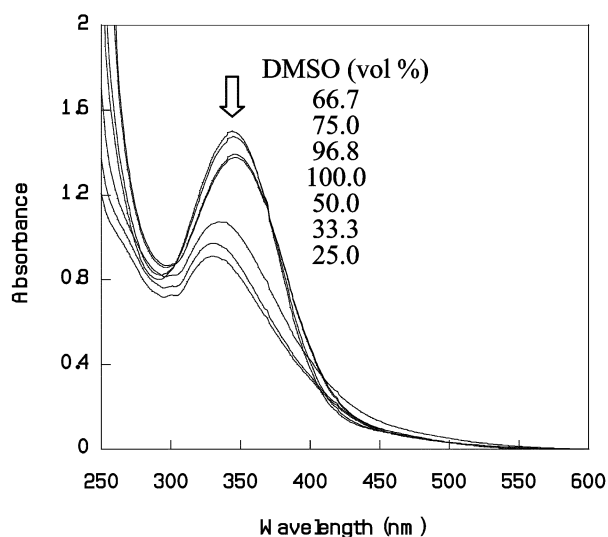


**Fig. 1** UV-Vis absorption spectra of **4** in DMSO–water mixtures: [**4**] =  $1.0 \times 10^{-4}$  mol dm<sup>-3</sup>, 0.5 cm cell, 20 °C.

The Soret band ( $\lambda_{\max}$  347 nm and  $\epsilon_{\max}$   $2.8 \times 10^4$  dm<sup>-3</sup> mol<sup>-1</sup> cm<sup>-1</sup> in DMSO) is scarcely affected at DMSO > 60 vol% whereas  $\lambda_{\max}$  shifts to shorter wavelength and the absorbance decreases at DMSO < 50 vol%.  $\lambda_{\max}$  is plotted against DMSO vol% for **1–4** in Fig. 2. It is seen from Fig. 2 that the  $\lambda_{\max}$  values are all similar in DMSO but shift to shorter wavelength with increasing water concentration. The  $\lambda_{\max}$  shift in 25 vol% DMSO appears (from the shorter wavelength) in the order of **4** > **3** > **1** > **2**. It is known that such a hypsochromic shift is

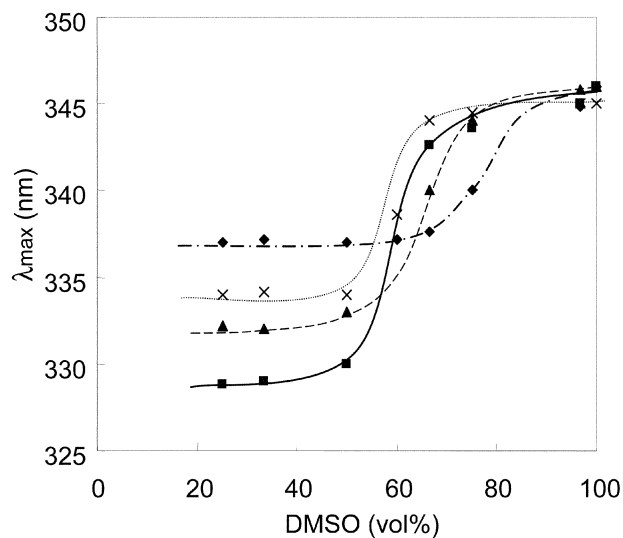


**Fig. 2**  $\lambda_{\max}$  of the Soret band plotted against DMSO vol% of **1** (----), **2** (—), **3** (.....) and **4** (—).

induced by H-type aggregation of chromophores.<sup>12</sup> The results imply, therefore, that the azobenzene moieties in **1–4** aggregate in a face-to-face manner and a transition from monomer to aggregate occurs at 60–80 vol% DMSO. Judging from the size of the shift, one may consider that the interaction in **4** is strongest.

CD spectra of **1–4** were measured in DMSO where they are dissolved discretely as monomers and in 50 vol% DMSO where

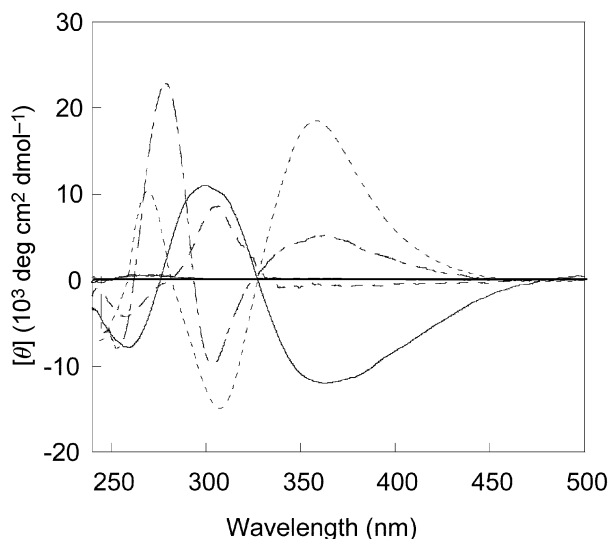


Fig. 3 CD spectra of **1** (-----), **2** (—), **3** (.....) and **4** (— · —) in 50 vol% DMSO:  $[1-4] = 1.0 \times 10^{-4} \text{ mol dm}^{-3}$ , 0.5 cm cell, 20 °C.

they form aggregates. The four compounds are all CD-silent in DMSO but become CD-active in 50 vol% DMSO (Fig. 3). The results show that these CD spectra do not arise from chirality in the monomeric species but from intermolecular dipole-dipole interactions in the aggregate species. As the isosbestic  $\lambda_{\theta=0}$  value (ca. 330 nm) in Fig. 3 is very close to the  $\lambda_{\text{max}}$  values of the UV-Vis absorption spectra (Fig. 2), one may consider that the CD bands in the 300–400 nm region are attributed to the exciton coupling bands. Thus, **1** and **2** which exhibit a first positive Cotton effect and a second negative Cotton effect tend to aggregate into the (*R*) helical direction whereas **3** and **4** which exhibit the opposite Cotton effects tend to aggregate into the (*S*) helical direction.

The foregoing results suggest that there is a significant spectroscopic difference between the **1** and **2** group and the **3** and **4** group. The difference is rationalized in terms of the absolute configuration in the sugar groups: that is, **1** and **2** have only equatorial OH groups whereas **3** and **4** have one axial OH group. This means that the presence of the axial OH group facilitates H-type aggregation and results in the (*S*) helical orientation. Taking these spectroscopic properties in solution into account, we investigated their gelation abilities and spectroscopic properties in the gel state.

### Gelation tests

The gelation abilities of **1–4** were evaluated in several organic solvents and water. The results are summarized in Table 1. It is seen from Table 1 that these bolaamphiphiles are insoluble in most organic solvents ('I' in Table 1). Even though they were dissolved at reflux temperature, they precipitated when they were cooled to room temperature ('P' in Table 1). On the other hand, they were soluble in DMF and DMSO. Here, an idea came to our mind that gelation would occur in appropriate DMF (or DMSO)–water mixtures. As expected, **1** bearing  $\beta$ -D-glucopyranosyl groups and **2** bearing  $\alpha$ -D-glucopyranosyl groups could gelate a 1:1 (v/v) DMSO–water mixture (Table 1). Surprisingly, **1** could gelate even water.<sup>13</sup> Thus, further gelation experiments were carried out in DMSO–water mixtures.

Table 2 summarizes the gelation abilities of **1** and **2** in various DMSO–water mixtures. **1** and **2** can gelate the mixtures in the range of 0–60 vol% DMSO and 40–80 vol% DMSO, respectively. Since the sol–gel phase-transition temperatures ( $T_{\text{gel}}$ : shown in parentheses) for **1** are generally higher than those for **2**, one may consider the **1** gels to be more stable than the **2** gels. It is particularly worth mentioning that the  $T_{\text{gel}}$  values determined in a sealed tube for **1** in the water-rich solvents are higher than the boiling point of water. To obtain a further insight into

Table 1 Results of gelation tests for **1–4**<sup>a</sup>

Solvent	Bolaamphiphile			
	<b>1</b>	<b>2</b>	<b>3</b>	<b>4</b>
Hexane	I	I	I	I
Benzene	I	I	I	I
Toluene	I	I	I	I
Chloroform	I	I	I	I
THF	I	I	I	I
Ethyl acetate	I	I	I	I
Acetone	I	I	I	I
Methanol	P	P	P	P
Ethanol	P	P	P	P
Benzyl alcohol	P	P	P	P
Acetonitrile	P	P	P	P
DMF	S	S	S	S
DMSO	S	S	S	S
DMSO–H <sub>2</sub> O = 1/1	G	G	P	P
Water	G	P	I	I

<sup>a</sup>  $[1-4] = 3.0 \text{ (wt/v)\%}$ ; G = transparent gel, S = clear solution after cooling, P = precipitation, I = insoluble.

Table 2 Gelation tests for **1** and **2** in DMSO–water mixtures and their  $T_{\text{gel}}$  values<sup>a</sup>

Solvent (vol%)		Bolaamphiphile <sup>b</sup>	
DMSO	Water	<b>1</b>	<b>2</b>
0	100	G (184)	P
20	80	G (167)	P
40	60	G (153)	G (79)
50	50	G (115)	G (77)
60	40	G (73)	G (68)
80	20	S	G (42)
100	0	S	S

<sup>a</sup>  $[1 \text{ or } 2] = 3.0 \text{ (wt/v)\%}$ . <sup>b</sup>  $T_{\text{gel}}$  values (°C) are shown in parentheses.

Table 3 Gelation ability of **1** and **2** in a 1:1 (v/v) DMSO–water mixture

Concentration (wt/v) %	Gelator	
	<b>1</b>	<b>2</b>
3.00	G (115) <sup>a</sup>	G (77) <sup>a</sup>
1.50	G	G
1.00	G	G
0.50	G	G
0.42	G	G
0.38	G	G
0.30	G	S
0.25	G	S
0.23	S	S

<sup>a</sup>  $T_{\text{gel}}$  (°C).

the gel stability the  $T_{\text{gel}}$  values were estimated as a function of their concentrations in a 1:1 (v/v) DMSO–water mixture (Table 3). As expected, the critical gelation concentration for **1** [0.25 (g ml<sup>-1</sup>) %] is lower than that for **2** [0.38 (g ml<sup>-1</sup>) %], indicating that **1** is classified as a better gelator than **2**.

From these results of gelation tests, we decided to estimate their morphological properties in a 1:1 (v/v) DMSO–water mixture where both **1** and **2** can result in stable translucent gels.

### Spectral and morphological properties of gels

The morphological structures of molecular assemblies constructed in organogels can be characterized by TEM and SEM observations. In the present system, however, the volatility of DMSO was so low that it was very difficult to prepare the fine xerogel samples suitable for TEM observation by a freezing-

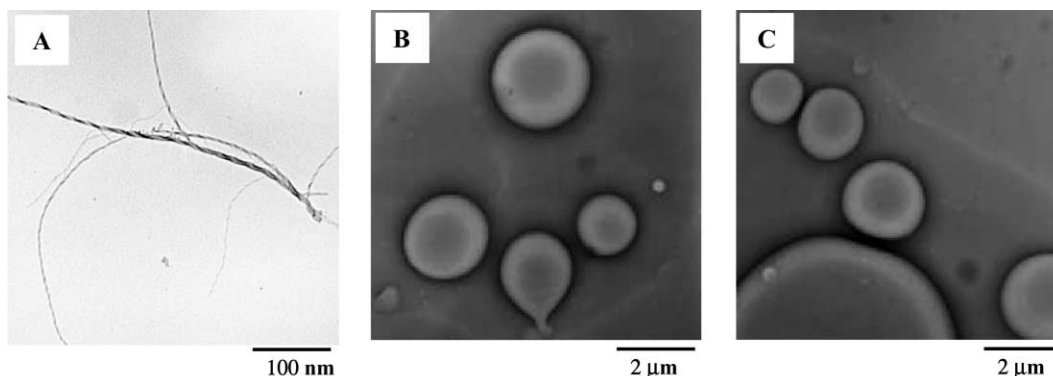


**Fig. 4** TEM images of **2** (A), **3** (B) and **4** (C) in 1:1 (v/v) DMSO–water mixtures. The sample for **2** ( $6.4 \times 10^{-3} \text{ mol dm}^{-3}$ ) was prepared by pouring the gel into acetone. The TEM image of **1** (not shown here) was basically similar to that of **2**. The samples for **3** and **4** ( $6.4 \times 10^{-3} \text{ mol dm}^{-3}$  each) were prepared from the top clear part of their precipitate mixtures. The samples were stained with uranyl acetate (2.0% aqueous solution).

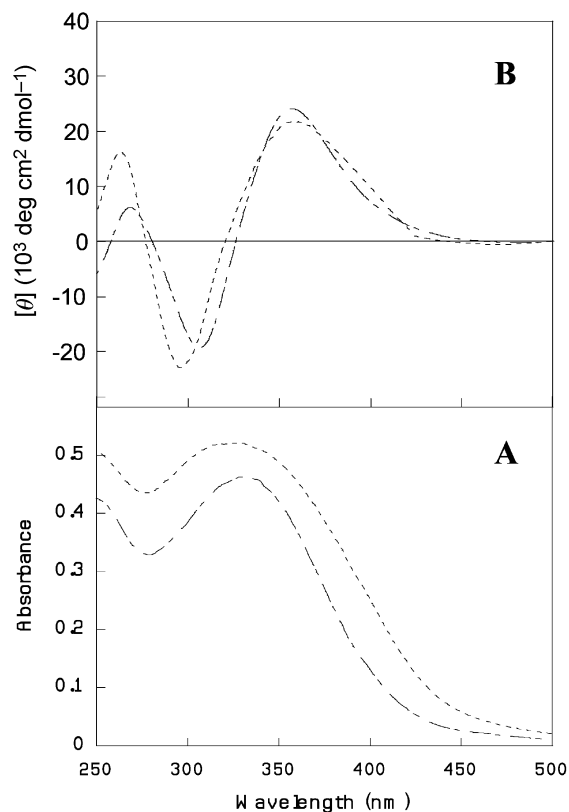


**Fig. 5** UV-Vis absorption (A) and CD (B) spectra of **1** (----), **2** (—) gels ( $6.4 \times 10^{-3} \text{ mol dm}^{-3}$ ) in 1:1 (v/v) DMSO–water mixtures: 0.05 mm cell, 20 °C.

and-pumping method. We poured the DMSO–water gel of **1** into acetone and the turbid mixture thus formed was deposited on the carbon mesh. The samples thus obtained were subjected to TEM observation.<sup>14</sup>

As shown in Fig. 4A, the fibrous helical structure was recognized in the TEM images of the samples prepared from the DMSO–water gels of both **1** and **2** [ $0.50 \text{ (g ml}^{-1}\text{) \%}$ ;  $6.4 \times 10^{-3} \text{ mol dm}^{-3}$ ]. The UV-Vis absorption and CD spectra of these DMSO–water gels are shown in Fig. 5. In the UV-Vis absorption spectra, the  $\lambda_{\text{max}}$  values (ca. 330 nm) are comparable with those of aggregated **1** and **2** in solution (Fig. 1), although the spectral shape is somewhat broadened. The CD spectra show exciton-coupling-type bands with a first positive Cotton effect and a second negative Cotton effect, which are also comparable with those of aggregated **1** and **2** in solution (Fig. 3). Since the LD (linear dichroism) spectra measured under the same conditions were negligibly small, one can regard that these spectra are assigned to the true CD spectra. These results suggest that the incipient aggregates formed in the solution grow up into

helical fibers in the gel state, maintaining the characteristic face-to-face (as shown by the hypsochromic shift), (*R*)-helical orientation (as shown by the sign of exciton coupling).

As summarized in Table 1, both **3** and **4** precipitated from the 1:1 (v/v) DMSO–water mixture. We therefore subjected their supernatants to TEM observation. As shown in pictures B and C in Fig. 4, they result in vesicular structures. This finding implies that **3** and **4** tend to aggregate into two-dimensional lamellar structures, which are favourable for vesicle formation but unfavourable for linear fiber formation. Thus, one can regard that the major reason why **3** and **4** cannot act as gelators is associated with their two-dimensional aggregation mode.<sup>15</sup>

#### Reversible morphology control

It is known that the vesicular aggregate can gradually change into a one-dimensional aggregate with a helical ribbon structure and eventually grow up into a tubular structure.<sup>16</sup> This tubular aggregate can be converted back to the vesicular aggregate only when it is heated above the phase-transition temperature.<sup>15</sup> Here, one interesting idea occurred to us: if the one-dimensional aggregate with the fibrous structure is perturbed by some appropriate additive, as perturbed by heating, it may be converted to the vesicular structure without changing the medium temperature. We previously found that boronic acid-appended poly(L-lysine) (**5**) efficiently interact with aggregates of various sugar-integrated amphiphiles.<sup>10,11</sup> We thus expected that the fibrous structure of **2** formed in the gel phase of a 1:1 (v/v) DMSO–water mixture might be perturbed by the addition of **5**.

Firstly, we measured the  $T_{\text{gel}}$  values against the concentration of added **5** ( $[\mathbf{2}] = 1.0 \times 10^{-2} \text{ mol dm}^{-3}$ ; Fig. 6). The  $T_{\text{gel}}$  in the

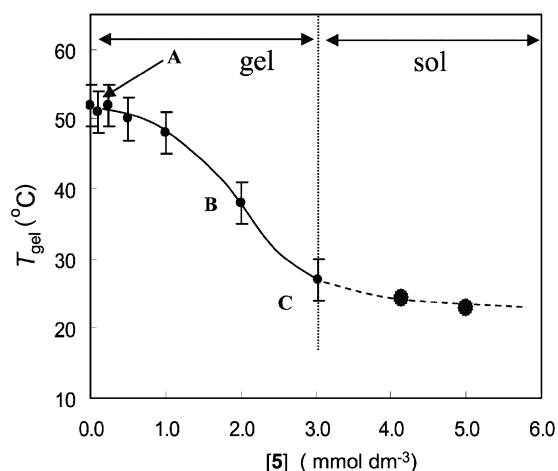


**Fig. 6** Plot of  $T_{\text{gel}}$  versus added **5**:  $[\mathbf{2}] = 1.0 \times 10^{-2} \text{ mol dm}^{-3}$ , 1:1 (v/v) DMSO–water mixture. The error bars indicate the range of reproducibility.

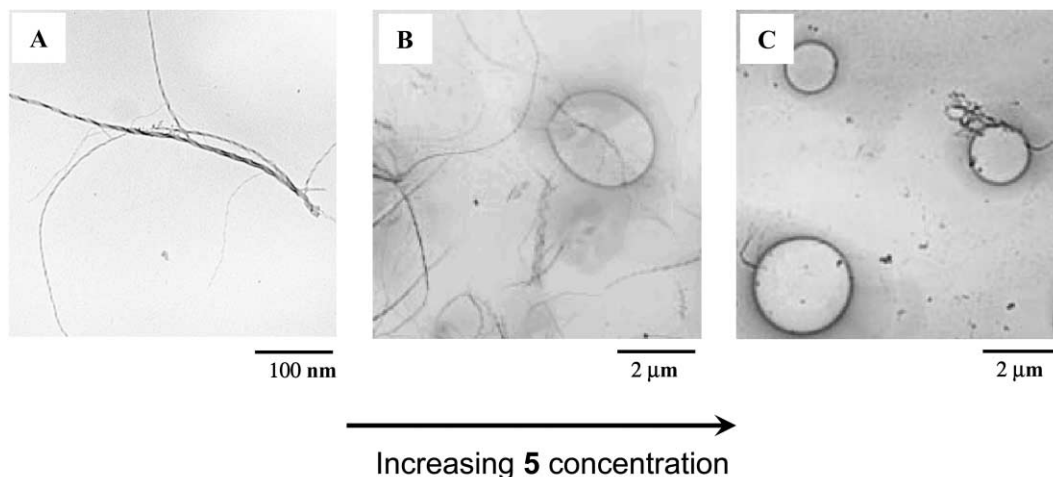


Fig. 7 TEM images of the aggregates prepared at A, B and C in Fig. 6.

absence of **5** is  $53 \pm 3$  °C. As shown in Fig. 6, the  $T_{\text{gel}}$  values decrease with increasing **5** concentration and above  $[\mathbf{5}] = 3.0$  monomer unit  $\text{mmol dm}^{-3}$  the gel phase changes into the sol phase. The results show that the fibrillar aggregate structure formed in the gel phase is destabilized by the boronic acid (in **5**)–diol (in **2**) interaction. To obtain insights into a morphological change induced by added **5** we took TEM pictures at the **5** concentrations A (in the absence of **5**), B ( $[\mathbf{5}] = 2.0$  monomer unit  $\text{mmol dm}^{-3}$ ) and C ( $[\mathbf{5}] = 3.0$  monomer unit  $\text{mmol dm}^{-3}$ ). At B, the 1:1 (v/v) DMSO–water mixture still maintains the gel state, but the TEM image shows the coexistence of the fibrillar structure and the vesicular structure (Fig. 7B). At C, where the mixture has been changed into the sol state, only the vesicular structure is recognized. The results indicate that the boronic acid–diol interaction between **5** and **2** is strong enough to destabilize the fibrillar structure and to induce the phase transition.

The above proposal implies that if the boronic acid–diol interaction between **5** and **2** is suppressed, the vesicular structure should be converted again back to the fibrillar structure. It is known that D-fructose possesses the highest affinity with the monoboronic acid group.<sup>6–9</sup> Thus, added D-fructose molecules should replace the diol groups in **2** complexed with the boronic acid groups in **5**, suppressing the interaction between **5** and **2**. Fig. 8 shows a plot of  $T_{\text{gel}}$  of the **5** + **2** gel versus added D-fructose concentration. The  $T_{\text{gel}}$  values increase with increasing added D-fructose concentration up to  $[\text{D-fructose}] = 5.0 \times 10^{-2}$   $\text{mol dm}^{-3}$  but gradually decrease at higher D-fructose

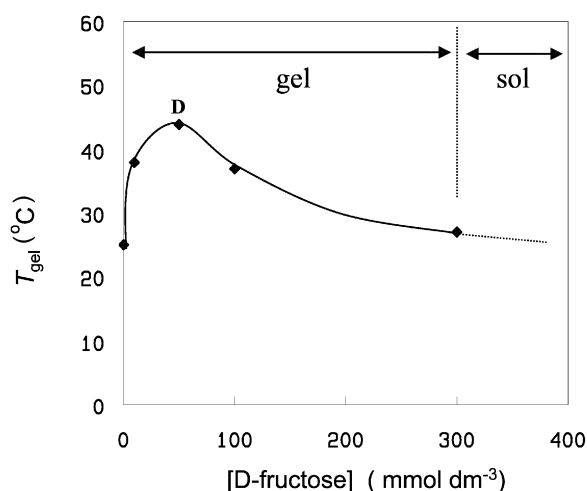


Fig. 8 Plot of  $T_{\text{gel}}$  of the **5** + **2** gel versus added D-fructose concentration:  $[\mathbf{5}] = 4.0 \times 10^{-3}$  monomer unit  $\text{mol dm}^{-3}$ ,  $[\mathbf{2}] = 1.0 \times 10^{-2}$   $\text{mol dm}^{-3}$ .

concentrations. This gel stabilization effect is due to the recovery of the sugar–sugar interaction in the fibrillar structure. On the other hand, the gel destabilization effect at higher D-fructose concentrations is due to the sugar–D-fructose interaction which intercepts the favorable sugar–sugar interaction in the fibrillar structure. At D in Fig. 8 ( $[\text{D-fructose}] = 5.0 \times 10^{-2}$   $\text{mol dm}^{-3}$  where the maximum  $T_{\text{gel}}$  was observed) we took a TEM picture. As shown in Fig. 9, a well-grown fiber structure is

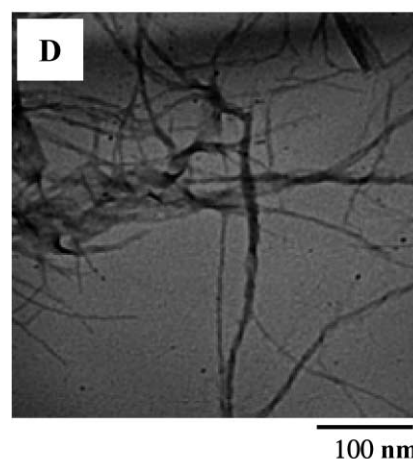


Fig. 9 TEM image of the sample prepared at D in Fig. 8.

observable, which is similar to those in Fig. 4A or Fig. 7A. One may consider, therefore, that the **5**–**2** interaction, which is the origin of the fiber structure destabilization, is suppressed by the predominant **5**–D-fructose interaction. The  $T_{\text{gel}}$  decrease at higher D-fructose concentrations in Fig. 8 is attributed to the interference with the hydrogen-bonding interaction among  $\alpha$ -D-glucopyranosyl groups in **2** by added D-fructose.

Thus the foregoing findings indicate that it is possible to reversibly control the sol–gel phase transition as well as the fiber–vesicle morphology transition by the addition of **5** or D-fructose.

### Concluding remarks

It is known that low molecular weight gelators mostly tend to aggregate in the one-dimensional direction. However, there is no general and firm principle for molecular design of such gelators. The present paper demonstrated that in bolaamphiphiles bearing two terminal sugar groups and one azobenzene segment, gelators can be found by combinatorial screening of the appropriate sugar groups from a carbohydrate family. In addition, one can obtain useful information from the spectroscopic properties of the azobenzene moiety on how

the molecules are assembled and how the gel is formed. One may consider, therefore, that this is a potential molecular design method to efficiently find versatile gelators and obtain 'feedback' information on the gelation mechanism. Furthermore, it was shown for the first time that the sol-gel phase transition as well as the vesicle-fiber transition can be reversibly controlled at the constant temperature by the interaction with **5** and D-fructose. The findings imply that this system is applicable as new functional materials, e.g., to sugar-triggered drug release, reversible encapsulation in vesicles, reinforcement of organogels, etc.

## Experimental

### Materials

Azobenzene-4,4'-dicarboxylic acid was purchased from Tokyo Chemical Industries, Ltd. and used without further purification. The preparations of 4-aminophenyl derivatives were reported previously.<sup>5</sup> The preparation of **5** was also reported previously.<sup>10,17</sup>

### 4,4'-[Bis( $\beta$ -D-glucopyranosyl)phenyl]azobenzene dicarboxamide (**1**)

Azobenzene-4,4'-dicarboxylic acid (300 mg, 1.11 mmol) was refluxed in thionyl chloride (8.1 ml, 111 mmol) containing a few drops of DMF under a nitrogen atmosphere for 2 h. The reaction mixture was concentrated to dryness under reduced pressure and the residue was dissolved in THF (15 ml). This solution was added dropwise to the stirred THF solution (15 ml) of 4-aminophenyl  $\beta$ -D-glucopyranoside (662 mg, 2.44 monomer unit mmol) and triethylamine (0.75 ml, 5.43 mmol) at 0 °C under nitrogen atmosphere. After stirring for 12 h at 40 °C, the reaction mixture was evaporated to dryness and the residue was dissolved in a small amount of DMSO. The solution was added to H<sub>2</sub>O and the precipitate was filtered: yield (655 mg, 76%), mp >300 °C (decomp.); (Found: C, 58.25; H, 5.23; N, 7.18. C<sub>38</sub>H<sub>40</sub>N<sub>4</sub>O<sub>14</sub>·0.4 H<sub>2</sub>O requires C, 58.22; H, 5.22; N, 7.15%);  $\delta_{\text{H}}$  (300 MHz; DMSO-*d*<sub>6</sub>, 298 K) 3.12–3.67 (12H, m, CH in sugar), 4.56 (2H, bs, OH in sugar), 4.79 (2H, d, *J* 7.0, OH in sugar), 5.12 (4H, bs, OH in sugar), 5.30 (2H, bs, OH in sugar), 7.01 (4H, d, *J* 7.8, ArH), 7.67 (4H, d, *J* 7.8, ArH), 8.03 (4H, d, *J* 7.5, ArH), 8.15 (4H, d, *J* 7.5, ArH), 10.34 (2H, bs, NHCO); SIMS (negative mode, 2-nitrobenzyl alcohol) *m/z* 776 (M – H).

The related compounds **2–4** were synthesized according to a similar method. We therefore describe only their analytical data.

### 4,4'-[Bis( $\alpha$ -D-glucopyranosyl)phenyl]azobenzene dicarboxamide (**2**)

Yield (638 mg, 74%), mp >300 °C (decomp.); (Found: C, 58.09; H, 5.21; N, 7.16. C<sub>38</sub>H<sub>40</sub>N<sub>4</sub>O<sub>14</sub>·0.3 H<sub>2</sub>O requires C, 58.35; H, 5.23; N, 7.16%);  $\delta_{\text{H}}$  (300 MHz; DMSO-*d*<sub>6</sub>, 298 K) 3.14–3.60 (12H, m, CH in sugar), 4.45 (2H, t, *J* 5.7, OH in sugar), 4.88 (2H, d, *J* 5.0, OH in sugar), 4.93 (2H, d, *J* 5.7, OH in sugar), 5.01 (2H, d, *J* 6.3, OH in sugar), 5.31 (2H, d, *J* 3.4, OH in sugar), 7.07 (4H, d, *J* 8.6, ArH), 7.67 (4H, d, *J* 8.6, ArH), 8.03 (4H, d, *J* 8.2, ArH), 8.15 (4H, d, *J* 8.2, ArH), 10.34 (2H, bs, NHCO); SIMS (negative mode, 2-nitrobenzyl alcohol) *m/z* 776 (M – H).

### 4,4'-[Bis( $\alpha$ -D-galactopyranosyl)phenyl]azobenzene dicarboxamide (**3**)

Yield (707 mg, 82%), mp >300 °C (decomp.); (Found: C, 58.11; H, 5.21; N, 7.21. C<sub>38</sub>H<sub>40</sub>N<sub>4</sub>O<sub>14</sub>·0.2 H<sub>2</sub>O requires C, 58.49; H, 5.22; N, 7.18%);  $\delta_{\text{H}}$  (300 MHz; DMSO-*d*<sub>6</sub>, 298 K) 3.31–3.77 (12H, m, CH in sugar), 4.50 (4H, m, OH in sugar), 4.69 (2H, d, *J* 4.1, OH in sugar), 4.84 (2H, d, *J* 5.3, OH in sugar), 5.34 (2H,

bs, OH in sugar), 7.06 (4H, d, *J* 8.6, ArH), 7.66 (4H, d, *J* 8.6, ArH), 8.02 (4H, d, *J* 8.2, ArH), 8.15 (4H, d, *J* 8.2, ArH), 10.32 (2H, bs, NHCO); SIMS (negative mode, 2-nitrobenzyl alcohol) *m/z* 776 (M – H).

### 4,4'-[Bis( $\alpha$ -D-mannopyranosyl)phenyl]azobenzene dicarboxamide (**4**)

Yield (672 mg, 78%), mp >300 °C (decomp.); (Found: C, 57.80; H, 5.25; N, 7.07. C<sub>38</sub>H<sub>40</sub>N<sub>4</sub>O<sub>14</sub>·0.6 H<sub>2</sub>O requires C, 57.82; H, 5.27; N, 7.11%);  $\delta_{\text{H}}$  (300 MHz; DMSO-*d*<sub>6</sub>, 298 K) 3.29–3.80 (12H, m, CH in sugar), 4.42 (2H, t, *J* 4.6, OH in sugar), 4.69 (2H, d, *J* 5.9, OH in sugar), 4.78 (2H, d, *J* 5.3, OH in sugar), 4.96 (2H, d, *J* 4.4, OH in sugar), 5.30 (2H, bs, OH in sugar), 7.07 (4H, d, *J* 8.6, ArH), 7.66 (4H, d, *J* 8.6, ArH), 8.03 (4H, d, *J* 8.2, ArH), 8.15 (4H, d, *J* 8.2, ArH), 10.33 (2H, bs, NHCO); SIMS (negative mode, 2-nitrobenzyl alcohol) *m/z* 776 (M – H).

### Solvent effect on gelation

The gelator and the solvent were put in a septum-capped sample tube and heated until the solid was dissolved. The solution was cooled at room temperature for 1 h. If the gel existed stably, it was classified as 'G' (Tables 2 and 3).

### Sol-gel phase-transition temperatures

The test tube containing the gel was immersed in a thermostatted oil bath. The temperature was raised at a rate of 2 °C min<sup>-1</sup>. Here, *T*<sub>gel</sub> is defined as the temperature at which the gel disappears.

### TEM observation

The sample was placed on a carbon-coated copper grid (400 mesh) and removed after the specimen was dried at low pressure. It was stained with 10–15  $\mu$ l drops of uranyl acetate (2.0 wt% aqueous solution). Then, this was dried for 1 h at low pressure. The specimen was examined with a Hitachi H-4500 microscope.

### Miscellaneous

<sup>1</sup>H NMR spectra were measured in DMSO-*d*<sub>6</sub> with a BRUKER ARX300 apparatus. IR spectra were recorded on a SHIMADZU FT-IR 8100M apparatus. CD spectra were measured on a JASCO J-720WI spectropolarimeter. The absorption spectra were measured by using a JASCO V-570 spectrophotometer.

## References

- For recent reviews see: (a) P. Terech and R. G. Weiss, *Chem. Rev.*, 1997, **97**, 3133; (b) J. H. van Esch and B. L. Feringa, *Angew. Chem., Int. Ed.*, 2000, **39**, 2263 and references therein; (c) R. J. H. Hafkamp, M. C. Feiters and R. J. M. Nolte, *J. Org. Chem.*, 1999, **64**, 412.
- (a) G. R. Newkome, G. R. Baker, S. Arai, M. J. Saunders, P. S. Russo, K. J. Theriot, C. N. Moorefield, L. E. Rogers, J. E. Miller, T. R. Lieux, M. E. Murray, B. Phillips and L. Pascal, *J. Am. Chem. Soc.*, 1990, **112**, 8458; (b) J.-H. Fuhrhop, J. S. Rosenberg and E. Boekema, *J. Am. Chem. Soc.*, 1987, **109**, 3387; (c) F. M. Menger and K. L. Caran, *J. Am. Chem. Soc.*, 2000, **122**, 11679; (d) R. Oda, I. Huc and S. J. Candau, *Angew. Chem., Int. Ed.*, 1998, **37**, 2689; (e) L. A. Estroff and A. D. Hamilton, *Angew. Chem., Int. Ed.*, 2000, **39**, 3447; (f) M. Jokić, J. Makarević and M. Žinić, *J. Chem. Soc., Chem. Commun.*, 1995, 1723; (g) U. Maitra, S. Mukhopadhyay, A. Sarkar, P. Rao and S. Indi, *Angew. Chem., Int. Ed.*, 2001, **40**, 2281.
- (a) S. Bhattacharya and S. N. Ghanashyam Acharya, *Chem. Mater.*, 1999, **11**, 3504; (b) J. H. Collier, B.-H. Hu, J. W. Ruberti, J. Zhang, P. Shum, D. H. Thompson and P. B. Messersmith, *J. Am. Chem. Soc.*, 2001, **123**, 9463.
- (a) O. Gronwald and S. Shinkai, *J. Chem. Soc., Perkin Trans. 2*, 2001, 1933; (b) O. Gronwald, K. Sakurai, R. Luboradzki, T. Kimura and S. Shinkai, *Carbohydr. Res.*, 2001, **331**, 307; (c) M. Amaike,

- H. Kobayashi and S. Shinkai, *Chem. Lett.*, 2001, 620; (d) N. Amanokura, Y. Kanekiyo, S. Shinkai and D. N. Reinhoudt, *J. Chem. Soc., Perkin Trans. 2*, 1999, 1995.
- 5 M. Amaike, H. Kobayashi and S. Shinkai, *Bull. Chem. Soc. Jpn.*, 2000, **73**, 2553.
- 6 (a) G. Wulff, *Pure Appl. Chem.*, 1982, **54**, 2093; (b) H. Matsubara, K. Seto, T. Tahara and S. Takahashi, *Bull. Chem. Soc. Jpn.*, 1986, **62**, 3896.
- 7 (a) Y. Shiomi, M. Saisho, K. Tsukagoshi and S. Shinkai, *J. Chem. Soc., Perkin Trans. 1*, 1993, 2111; (b) T. D. James, K. R. A. S. Sandanayake and S. Shinkai, *Angew. Chem., Int. Ed. Engl.*, 1994, **33**, 2207; (c) T. Imada, H. Murakami and S. Shinkai, *J. Chem. Soc., Chem. Commun.*, 1994, 1557; (d) T. D. James, K. R. A. S. Sandanayake and S. Shinkai, *Supramol. Chem.*, 1995, **6**, 141; (e) M. Takeuchi, K. Koumoto, M. Goto and S. Shinkai, *Tetrahedron*, 1996, **52**, 12931; (f) T. D. James, K. R. A. S. Sandanayake and S. Shinkai, *Angew. Chem., Int. Ed. Engl.*, 1996, **35**, 1910.
- 8 (a) J. Yoon and A. W. Czarnik, *J. Am. Chem. Soc.*, 1992, **114**, 5874; (b) L. K. Mohler and A. W. Czarnik, *J. Am. Chem. Soc.*, 1993, **115**, 2998; (c) M. F. Paugan and B. D. Smith, *Tetrahedron Lett.*, 1993, **34**, 3723; (d) G. T. Morin, M. P. Hughes, M.-F. Paugam and B. D. Smith, *J. Am. Chem. Soc.*, 1994, **116**, 8895; (e) P. R. Westmark and B. D. Smith, *J. Am. Chem. Soc.*, 1994, **116**, 9343; (f) Y. Nagai, K. Kobayashi, H. Toi and Y. Aoyama, *Bull. Chem. Soc. Jpn.*, 1993, **66**, 2965.
- 9 (a) G. Wulff, B. Heide and G. Helfmeier, *J. Am. Chem. Soc.*, 1986, **108**, 1089; (b) G. Wulff and H.-G. Poll, *Makromol. Chem.*, 1987, **188**, 741.
- 10 (a) T. Nagasaki, T. Kimura, S. Arimori and S. Shinkai, *Chem. Lett.*, 1994, 1495; (b) T. Kimura, M. Takeuchi, T. Nagasaki and S. Shinkai, *Tetrahedron Lett.*, 1995, **36**, 559; (c) T. Kimura, S. Arimori, M. Takeuchi, T. Nagasaki and S. Shinkai, *J. Chem. Soc., Perkin Trans. 2*, 1995, 1889; (d) H. Kobayashi, K. Nakashima, E. Ohshima, Y. Hisaeda, I. Hamachi and S. Shinkai, *J. Chem. Soc., Perkin Trans. 2*, 2000, 997.
- 11 H. Kobayashi, M. Amaike, J. H. Jung, A. Friggeri, S. Shinkai and D. N. Reinhoudt, *Chem. Commun.*, 2001, 1038.
- 12 (a) N. Harada and K. Nakanishi, *Acc. Chem. Res.*, 1972, **5**, 257; (b) T. Kunitake, *New J. Chem.*, 1987, **11**, 139; (c) T. Kunitake, *Angew. Chem., Int. Ed. Engl.*, 1992, **31**, 709.
- 13 The gelation properties of **1** as a hydrogelator has been published separately as a communication: H. Kobayashi, A. Friggeri, K. Koumoto, M. Amaike, S. Shinkai and D. N. Reinhoudt, *Org. Lett.*, 2002, **4**, 1423. In the caption to Fig. 4 of this article, 'solid line' and 'broken line' should be exchanged.
- 14 We understand that this method (to pour the sample into acetone) is a little risky. Thus, we have confirmed that (1) the freezing-and-pumping method, without using acetone, which takes a long time (about 3 days), results in the basically same morphological structures and (2) the gelator is not detectable in the acetone solution by a UV-Vis spectroscopic method.
- 15 R. Luboradzki, O. Gronwald, M. Ikeda, S. Shinkai and D. N. Reinhoudt, *Tetrahedron*, 2000, **56**, 9595. The UV-Vis and CD spectra of the supernatants were similar to those shown in Figs. 1 and 3, although they were somewhat broadened.
- 16 (a) N. Nakashima, S. Asakuma and T. Kunitake, *J. Am. Chem. Soc.*, 1985, **107**, 509; (b) J.-H. Fuhrhop and J. Koning, *Membranes and Molecular Assemblies*, The Royal Society of Chemistry, Cambridge, 1994.
- 17 H. Kobayashi, M. Amaike, K. Koumoto and S. Shinkai, *Bull. Chem. Soc. Jpn.*, 2001, **74**, 1311.